

# SPECIFICATION OF INPUTS AND INSTRUMENTATION FOR FLUTTER TESTING OF MULTIVARIABLE SYSTEMS

Narendra K. Gupta and W. Earl Hall, Jr.  
Systems Control, Inc.

## SUMMARY

This paper deals with the application of system identification methods in flutter testing of aeroelastic structures. The accuracy with which flutter parameters are estimated depends upon the test plan and on the algorithms used to reduce the data. The techniques for selecting the kinds and optimal positions of inputs and instrumentation, under typical test constraints, are presented. Identification results for both the input/output transfer function and the values of physical parameters are presented. Numerical results on the optimal input spectrum and the accelerometer location for estimating flutter parameters of a two dimensional wing are obtained using these algorithms. Current work on applying system identification methods to high order three dimensional aeroelastic structures is discussed.

## INTRODUCTION

The objective of flutter analysis is to quantify the critical points or boundaries of flutter and the stability margins associated with subcritical responses. While it is true that analytical predictive techniques have become increasingly useful to this objective, actual testing and data analysis is always required for verification of these analyses, or to provide results where analytical assumptions are suspect. Thus, flutter test analysis techniques are being developed which use experimental data (usually noisy) to provide accurate estimates of both subcritical stability margins as well as aid extrapolation to the critical points (refs. 1 and 2). To be most useful, these techniques should provide real time (or near real time) estimates to keep test times at a minimum.

Further requirements on these test analysis techniques are emerging due to new aircraft concepts. New structural concepts, such as light weight composites technology, and control concepts, such as the active control of maneuver loads and flutter margins, will require multivariable testing analysis methods. These multivariable analysis techniques are necessary to define the modal frequencies and damping of many interactive structural components in complex aerodynamic regimes.

To meet the challenging requirements of estimating accurate subcritical flutter test parameters and to use these results to effectively predict flutter boundaries for multivariable systems, a systematic approach must be adopted. This approach should integrate the specification of test instrumentation and inputs with multiinput/multioutput data analysis procedures.

The key elements of such an aeroelastic integrated testing analysis of a model or of a prototype vehicle are shown in figure 1. First, the test objective must be quantified. Historically, this test objective has progressed from finding the flutter boundary to more current determination of the frequency and damping of the subcritical stability margin. The need to be able to better use subcritical data to predict the boundary requires determination of the parameters of a flutter model which may contain two or more states of the system. Of course, accuracy specifications for these various levels must be set. Second, the operating points (of a wind tunnel or flight regime) must be set to provide the basis for meeting the objectives within test safety constraints.

To implement the test objectives at the required points, an extensive analysis of test inputs and instrumentation will minimize the probability of ineffective results due to the improper excitation of critical modes and low signal/noise ratios. With the test configuration specified, the data are collected and analyzed using either a spectral analysis technique (e.g., fast Fourier transform (FFT, ref. 3) or Randomdec (ref. 4)) or an advanced parameter identification algorithm.

This paper focuses on the specification of test inputs and instrumentation. Specifically, the three major elements of the test configuration are:

- (a) Choice and location of instruments (e.g., accelerometers, strain gages, gyros).
- (b) Choice of inputs with respect to type (e.g., sinusoidal, swept sines, random), and location of inputs and frequencies, and energy of inputs.
- (c) Required capability of test analysis procedures.

Analytical methods for input design and instrument selection to obtain the most accurate estimates of parameters in models describing the flutter behavior of aerodynamic structures are developed. The methods, based on system identification technology, minimize the expected covariance of errors in estimates of unknown parameters. The locations of the instruments and the inputs (if variable) may also be optimally selected.

This paper describes a simple model of an aeroelastic wing. The dynamics of the wing can be formulated as a state variable model. The analytical formulation of the input design problem for state variable models with unknown parameters is given, along with a description of the methods used for selecting the kind, accuracy, and locations of instruments. Some results on the selections of instruments and inputs to accurately identify the flutter characteristics of a two dimensional wing are described. Finally, the techniques are applied to large aerodynamic structures and the conclusions drawn from this work are discussed.

# STATE SPACE EQUATIONS FOR A TWO DIMENSIONAL WING IN FLUTTER

Flutter is an interaction between nonsteady aerodynamic forces and elastic forces in a structural component. To study the experimental design techniques for flutter testing, a reference model for the flutter of a two dimensional wing is given based on the work of Houbolt (ref. 5). The symbols used follow those of reference 5.

An oscillating two dimensional airfoil in an incompressible flow can be modeled as shown in figure 2. Various forces acting on the airfoil are: (a) lift  $L_1$  at quarter chord and lift  $L_2$  at three-quarter chord, (b) restoring force and moment through the elastic axis located at (a), (c) force and moment associated with the inertia of the substance constituting the medium (these will be neglected), and (d) external forces and/or moments, used to excite flutter or inadvertently transmitted through the structure. The lifts  $L_1$  and  $L_2$  are modeled with appropriate delays. Houbolt (ref. 5) shows that the aero-elastic equations for the wing can be written in terms of nondimensional variables as follows (see also fig. 2):

$$\begin{bmatrix} \mu s^2 + \mu \omega_y^2 & -\mu r s^2 - \frac{1}{2} s & -1 \\ -\mu r s^2 & \mu \frac{k_m^2}{c^2} s^2 + \frac{1}{2} r_2 s + \mu \frac{k_m^2}{c^2} \omega_\phi^2 & -r_1 \\ 2a_2 s^2 + 2b_2 s & -2r_2 a_2 s^2 - (a_2 + 2b_2 r_2) s - b_2 & s + b_2 \end{bmatrix} \begin{bmatrix} w \\ \phi \\ u \end{bmatrix} = \begin{bmatrix} 1 \\ r_f \\ 0 \end{bmatrix} \bar{F} \quad (1)$$

By defining

$$w_1 \triangleq \dot{w}$$

$$\phi_1 \triangleq \dot{\phi}$$

equation (1) becomes

$$\begin{bmatrix} \mu & -\mu r & 0 \\ -\mu r & \mu \frac{k_m^2}{c^2} & 0 \\ 2a_2 & -2r_2 a_2 & 1 \end{bmatrix} \begin{bmatrix} \dot{w}_1 \\ \dot{\phi}_1 \\ \dot{u} \end{bmatrix} = - \begin{bmatrix} \frac{-2}{\mu \omega_y^2} & 0 \\ 0 & \mu \frac{k_m^2}{c^2} \frac{-2}{\omega_\phi^2} \\ 0 & -b_2 \end{bmatrix} \begin{bmatrix} w \\ \phi \end{bmatrix} \\
 - \begin{bmatrix} 0 & -\frac{1}{2} & -1 \\ 0 & \frac{1}{2} r_2 & -r_1 \\ 2b_2 & -(a_2 + 2b_2 r_2) & b_2 \end{bmatrix} \begin{bmatrix} w_1 \\ \phi_1 \\ u \end{bmatrix} + \begin{bmatrix} 1 \\ r_f \\ 0 \end{bmatrix} \bar{F}$$

or

$$A_1 \begin{bmatrix} \dot{w}_1 \\ \dot{\phi}_1 \\ \dot{u} \end{bmatrix} = A_2 \begin{bmatrix} w \\ \phi \end{bmatrix} + A_3 \begin{bmatrix} w_1 \\ \phi_1 \\ u \end{bmatrix} + A_4 \bar{F} \quad (2)$$

Therefore

$$\frac{d}{dp} \begin{bmatrix} w_1 \\ \phi_1 \\ u \\ w \\ \phi \end{bmatrix} = \begin{bmatrix} A_1^{-1} A_2 & A_1^{-1} A_3 \\ I & 0 \end{bmatrix} \begin{bmatrix} w_1 \\ \phi_1 \\ u \\ w \\ \phi \end{bmatrix} + \begin{bmatrix} A_1^{-1} A_4 \\ 0 \end{bmatrix} \bar{F} \quad (3)$$

where I is an identity matrix. This is the state space representation of an aeroelastic wing and can be written compactly as

$$\dot{x} = Fx + Gu \quad (4)$$

where x is the state vector, u is the input vector, and F and G are transition matrices which contain unknown parameters. An accelerometer placed at  $e_o$  will measure

$$\begin{aligned} y &= \ddot{w} + \frac{e_o}{c} \ddot{\phi} \\ &= \dot{w}_1 + \frac{e_o}{c} \dot{\phi}_1 \end{aligned} \quad (5)$$

The quantities  $\dot{w}_1$  and  $\dot{\phi}_1$  can be expressed in terms of x using equation (3). Then

$$y = Hx + Du \quad (6)$$

The transfer function between y and u is

$$\begin{aligned} \frac{y(s)}{u(s)} &= H(sI - F)^{-1}G + D \\ &= \frac{b_4 s^4 + b_3 s^3 + b_2 s^2 + b_1 s + b_0}{s^5 + a_4 s^4 + a_3 s^3 + a_2 s^2 + a_1 s + a_0} + D, \quad s = j\omega \end{aligned} \quad (7)$$

This transfer function can be written again into a state space form, often referred to as a canonical form.

#### OPTIMAL SELECTION AND LOCATION OF INPUTS AND INSTRUMENTS

As shown above, the flutter equations of a wing can be written in either the state variable form or the transfer function form. The multivariable state equations and measurement equations are equations (4) and (6). In practice, the measurements, y, are corrupted by additive noise, v, so that

$$y = Hx + Du + v \quad (8)$$

where  $v$  is assumed to be a white noise source with power spectral density matrix  $R$ . The unknown parameters and some control parameters (locations of inputs and instruments) are imbedded in the matrices  $F$ ,  $G$ , and  $H$ . The unknown parameters, whose estimated we are interested in, will be denoted by  $\theta$ .

The accuracy of the parameter estimate  $\theta$  is expressed in terms of the bias and covariance properties of the estimate. It is assumed that an unbiased and efficient estimation procedure is used so that the input design and instrument selection can be carried out independently of the estimation procedure. This makes it possible to compute errors in the parameter estimates based on the Cramer-Rao lower bound. This bound is computed around an a priori value  $\theta_0$  for the parameters  $\theta$ . The information matrix  $M$  is related to the error in estimated by the following relation

$$\text{cov}(\theta - \hat{\theta}) \geq M^{-1} \quad (9)$$

where  $\hat{\theta}$  is the estimate of  $\theta$ .

The information matrix depends upon the input energy distribution and its location and instrument accuracies and their locations. The design procedures presented here will work with the properties of the information matrix. For physical reasons, a quadratic constraint is placed on the inputs and the state variables

$$\lim_{T \rightarrow \infty} \frac{1}{T} \int_0^T (x^T A x + u^T u) dt \leq E \quad (10)$$

where  $A$  is a symmetric positive semidefinite matrix. An equation for the information matrix, under the constraint of equation (10), in the frequency domain is now obtained.

#### Information Matrix in the Frequency Domain

The relation between  $y$  and  $u$  in frequency domain is

$$y(\omega) = \{H(j\omega I - F)^{-1}G + D\} u(\omega) \\ \triangleq T(\omega, \theta) u(\omega) \quad (11)$$

where  $T(\omega, \theta)$  is the transfer function from the input,  $u(\omega)$ , to the measurement  $y(\omega)$ .

Equation (10) is written in the frequency domain as

$$\int_0^{\infty} \{u(\omega) u^*(\omega) + \text{Tr}(Ax(\omega) x^*(\omega))\} d\omega \leq E \quad (12)$$

where  $\text{Tr}$  is the trace operator and '\*' denotes conjugate transpose. If  $S(\omega, \theta)$  is the transfer function between  $x$  and  $u$ , equation (12) may be written as

$$\int_0^{\infty} \{1 + \text{Tr}(A S(\omega, \theta) S^*(\omega, \theta))\} u(\omega) u^*(\omega) d\omega \leq E$$

or

$$\int_0^{\infty} \lambda(\omega, \theta) u(\omega) u^*(\omega) d\omega = E \quad (13)$$

The inequality sign can be removed for linear systems because increasing the input amplitude will increase the accuracy of all parameters. The information matrix for parameters  $\theta$  from measurements  $y$ , per unit time, is as follows (see refs. 6 and 7 for details):

$$M = \text{Re} \int_0^{\infty} \frac{\partial T}{\partial \theta}^* R^{-1} \frac{\partial T}{\partial \theta} u(\omega) u^*(\omega) d\omega \quad (14)$$

Defining

$$\bar{u}(\omega) \triangleq \lambda^{\frac{1}{2}}(\omega, \theta) u(\omega) \quad (15)$$

Equations (13) and (14) become

$$\int_0^{\infty} \bar{u}(\omega) \bar{u}^*(\omega) d\omega = E$$

$$M = \text{Re} \int_0^{\infty} \frac{\partial T^*}{\partial \theta} R^{-1} \frac{\partial T}{\partial \theta} \frac{1}{\lambda(\omega, \theta)} \bar{u}(\omega) \bar{u}^*(\omega) d\omega \quad (16)$$

The information matrix,  $M$ , serves as the basic quantity upon which the input and instrumentation requirements are to be determined. Maximizing  $M$  by appropriate input and instrumentation design parameters leads to output data which have a high information content on the system parameters. That is, the sensitivity of the outputs to parameters, for example, is maximized by exciting the modes which are most affected by the parameters. Basing the design on  $M$ , though mathematically simpler, has some disadvantages in practice. If the trace of  $M$  (e.g., the sum of diagonal elements) is maximized, an almost singular information matrix may result. The inverse of  $M$  is the lower bound on the parameter covariance matrix. If  $M$  is nearly singular, its inverse may contain large diagonal elements, leading to large errors in the estimates.

For this reason, it is more desirable to work directly with the inverse of the information matrix,  $M^{-1}$ . This matrix can be viewed as the ellipsoid of uncertainty of the parameters. Though mathematically more difficult to minimize, this matrix gives useful results since we are minimizing the parameter covariances directly. Two types of methods can be used to minimize  $M^{-1}$ . These are based on the following functions of  $M^{-1}$ :

- (1) Minimize  $\text{Det } (M^{-1})$ : This method will minimize the volume of the uncertainty ellipsoid. This also minimizes maximum error in the estimate of the transfer function.
- (2) Minimize  $\text{Tr } (WM^{-1})$ : This method minimizes a weighted sum of the parameter estimate covariances ( $W$  is the weighting matrix which penalizes certain estimate errors more heavily than others). The weighting matrix serves two purposes. Since the covariances of different parameters have different units, the weighting matrix converts each term in the sum to the same units. Secondly, the weighting matrix offers tremendous flexibility because it is possible to assign varying importance to parameters through weights on their nondimensional covariance. This is considered to be one of the most suitable performance criteria, since it works with parameter estimate covariances directly.



## Choice and Location of Optimal Input

The optimal input possesses certain properties which are quite important. They are presented here without proof (ref. 6):

- (1) The optimal input has a discrete spectrum (or point spectrum). The number of frequencies with nonzero power does not exceed  $\frac{m(m+1)}{2}$  where  $m$  is the number of parameters.
- (2) If the spectrum of  $u$  contains fewer than  $m/(2p)$  frequencies, the information matrix is singular (i.e., all the parameters cannot be identified).
- (3) The optimal input which minimizes  $\text{Det}(M^{-1})$  satisfies a minimum output error criterion. In other words, this input gives the best estimate of the transfer function.
- (4) They satisfy two important theorems (see refs. 6 to 8), which convert this complex nonlinear problem into a computation technique.

It has been demonstrated that the computation procedure summarized in appendix A can be applied to select the input spectrum which gives the desired minimum of  $M^{-1}$ .

Practical considerations in the computation of optimal input.— The algorithm of appendix A will produce an optimal input design with a sufficient number of iterations. However, at each iteration, the procedure adds one point to the spectrum of the input. For practical implementation, it is desirable to have as few frequencies in the optimal input as possible. During the computation, a few steps can be taken to reduce the number of points in the spectrum. Suppose the normalized input at any stage has  $k$  frequencies  $\omega_i$  with power  $\alpha_i$  ( $i=1,2,\dots,k$ ). Then:

- (a) Frequencies less than  $\Delta\omega$  apart can be lumped into one frequency. Suppose  $q$  frequencies  $\omega_i^*$  are within a band  $\Delta\omega$  wide. Then they can be replaced by one frequency  $\omega^*$  with power  $\alpha^*$  where

$$\alpha^* = \sum_{i=1}^q \alpha_i^*$$

and

$$\omega^* = \frac{1}{\alpha^*} \sum_{i=1}^q \alpha_i^* \omega_i^*$$

(17)

- (b) From this new input, all frequencies  $\omega_i$  with power less than a threshold  $\alpha'$  are dropped. The remaining frequencies do not satisfy the constraint of equation (13), so the design is renormalized.

Steps (a) and (b) should be carried out to ensure that the design does not become degenerate. This "practicalization" requires judgment of  $\Delta\omega$  and  $\alpha$ .

Choice of location of input.— The transfer functions  $T(\omega, \theta)$  (the input-to-output transfer function) and  $S(\omega, \theta)$  (the input-to-state transfer function) are both linear functions of the control distribution matrix  $G$ . The location of the input affects  $G$  in a linear fashion. Therefore, if  $\beta$  is an input location parameter, the transfer functions  $T(\omega, \theta)$  and  $S(\omega, \theta)$  can be written as

$$\begin{aligned} T(\omega, \theta) &= T_1(\omega, \theta) + \beta T_2(\omega, \theta) \\ S(\omega, \theta) &= S_1(\omega, \theta) + \beta S_2(\omega, \theta) \quad , \quad 0 \leq \beta \leq 1 \end{aligned} \tag{18}$$

Equations (13) and (14) can, therefore, be written as

$$\int_0^\infty \{1 + \text{Tr}(A(S_1(\omega, \theta) + \beta S_2(\omega, \theta)) (S_1(\omega, \theta) + \beta S_2(\omega, \theta))^*)\} u(\omega) u^*(\omega) d\omega = E$$

i.e.,

$$\gamma(1 + c_1\beta + c_2\beta^2) = E \tag{19}$$

and

$$M = \gamma[M_{11} + 2\beta M_{12} + \beta^2 M_{22}] \tag{20}$$

$\gamma$  is a scalar which adjusts the energy in the input to satisfy the quadratic constraint on the input and the states. Equations (19) and (20) can be combined into one equation,

$$M = \frac{E}{1 + c_1\beta + c_2\beta^2} [M_{11} + 2\beta M_{12} + \beta^2 M_{22}] \quad , \quad 0 \leq \beta \leq 1 \tag{21}$$

$\beta$  can be selected to minimize  $|M^{-1}|$  or  $\text{Tr}(WM^{-1})$ . In fact, an algorithm similar to that of appendix A for input frequency and power selection can be developed.

In a more general case, when there is more than one input and each input may be placed over any point in two or more dimensions, the number of parameters  $\beta$  which must be selected optimally is more than one. The optimization becomes somewhat more difficult, but the basic approach remains the same.

### Choice and Location of the Instruments

In addition to selecting the location and type of the excitation signal, there are two other design considerations in planning a flutter test. These are the determination of the kind of instruments which must be used to record flutter response and the choice of instrument location (if there is a choice). Though the problem of instrument selection and location can be treated simultaneously, for sake of simplicity we treat them separately.

Selection of instruments.— The selection of instruments is a tradeoff between dynamic range, accuracy, and cost. The dynamic loads are often limited by structural constraints, and it will be assumed that the instruments cover this range. The accuracy with which the parameters may be estimated is then determined by the accuracy of the instruments. It is clear from equation (14) that the information matrix has an inverse relationship with the measurement noise covariances.

$$M = \text{Re} \int_0^{\infty} \frac{\partial T^*}{\partial \theta} R^{-1} \frac{\partial T}{\partial \theta} u(\omega) u^*(\omega) d\omega \quad (22)$$

For the purpose of instrument selection in general, the measurement noise covariance matrix is diagonal, i.e.,

$$R^{-1} = \text{diag}[r_{11}, r_{22}, \dots, r_{pp}] \quad (23)$$

where  $1/r_{11}$  is the covariance of random noise in the  $i$ th instrument. The total cost of the  $p$  instruments is a sum of the cost of individual instruments

$$C = \sum_{i=1}^p C_i(r_{ii}) \quad (24)$$

The total cost of the instrument package is assumed to be fixed. Either of the criteria of equation (17) may be minimized under the cost constraint and

$$r_{ii} \geq 0 \quad i=1,2,\dots,p. \quad (25)$$

The Lagrange multiplier approach may be used for optimization. For example, if the criterion requires the minimization of  $|M^{-1}|$ , the modified cost function is

$$\bar{J} = |M^{-1}| + \sum_{i=1}^p (\lambda_i r_{ii} - \mu C_i(r_{ii})) + \mu C \quad (26)$$

where  $\lambda_i$ ,  $i=1,2,\dots,p$ , and  $\mu$  are Lagrange multipliers. The following optimization equations result:

$$r_{ii} = 0 \quad , \quad \text{or} \quad \lambda_i = 0$$

$$|M|^2 \text{Tr} \left\{ M^{-1} \frac{\partial M}{\partial r_{ii}} \right\} + \lambda_i - \mu \frac{\partial C_i}{\partial r_{ii}} = 0 \quad , \quad i=1,2,\dots,p. \quad (27)$$

Equations (24) and (27) are  $2p+1$  equations in  $2p+1$  unknowns  $\lambda_i$ ,  $r_{ii}$  and  $\mu$ . Note that if any  $r_{ii}$  is zero, the corresponding instrument has infinite error; in other words, this instrument should not be used.

The optimal value of  $r_{ii}$  would act as a guideline in selecting the instrument. Often, it is not possible to obtain an instrument with mean square error of  $\frac{1}{r_{ii}}$  exactly and cost  $C_i(r_{ii})$ .

Location of instruments.— The transfer function  $T(\omega, \theta)$  is a linear function of the measurement distribution matrix  $H$ , and, therefore, the position of the instrument. For this reason, optimal choice of instrument location can be determined in the same way as the optimal positioning of inputs.

## RESULTS

To demonstrate the application of the methods described above to multi-variable flutter problems, a two dimensional wing is considered. The values of the parameters are as follows:  $\mu = 10$ ,  $(k_m^2/c^2) = \alpha = 0.1$ ,  $a/c = 0.35$ ,  $r_1 = 0.1$ ,  $r_2 = 0.4$ ,  $a_2 = 0.6$ , and  $b_2 = 0.3$ . The velocity is taken as 15.25c meters/sec (50c ft/sec) and the natural frequencies of the rotational and ver-

tical motions are 10 hertz and 2 hertz, respectively. This gives the system matrices for the nondimensional state equations as

$$F = \begin{bmatrix} 0 & 0.05 & 0.1 & \underline{-0.01579} & 0 \\ 0 & \underline{-0.2} & \underline{0.1} & 0 & \underline{-0.3948} \\ \underline{-0.6} & 0.684 & \underline{-0.372} & \underline{0.01895} & 0.1105 \\ 1 & 0 & 0 & 0 & 0 \\ 0 & 1 & 0 & 0 & 0 \end{bmatrix} \quad (27)$$

and

$$G^T = [0.1, \frac{e_f}{c}, \underline{-0.12 - 0.48 \frac{e_f}{c}}, 0, 0] \quad (28)$$

The measurement distribution matrices are

$$H = [0, 0.5 - 0.2 \frac{e_o}{c}, 0.1 + 0.1 \frac{e_o}{c}, -0.01579, -0.3948 \frac{e_o}{c}] \quad (29)$$

$$D = (0.1 + \frac{e_f}{e_c} \cdot \frac{e_o}{c})$$

where  $\frac{e_f}{c}$  and  $\frac{e_o}{c}$  are parameters which define the locations of the input actuator and the accelerometer. The noise in the accelerometer is assumed to be white, with a standard deviation of 0.02 in dimensionless units (this corresponds to about 0.61 meters/sec/sec (2 ft/sec/sec)) and a sampling interval of 4 milliseconds. It is assumed that we are interested in estimating the parameters  $\omega_y^{-2}$ ,  $\omega_\phi^{-2}$ ,  $r_2$ ,  $a_2$ ,  $b_2$ ,  $\alpha$ .

The poles and zeros of the transfer function between the measurement and the input  $\frac{e_f}{c}$  and  $\frac{e_o}{c}$  both equal to 0.1, are, in radians per second (the nondimensional values are multiplied by 100)

$$\begin{array}{ll}
\text{Poles} & -5.76 \pm 55.6j \\
& -19.4 \pm 16.6j \\
& -6.83 \\
\text{Zeros} & -0.163 \pm 76.2j \\
& -30.0 \\
& -5.68
\end{array} \tag{30}$$

### Input Design

As mentioned before, the inputs are designed to maximize the identifiability of flutter parameters from output. The test duration was selected as 2 seconds. This is a fairly short test, but in terms of the natural frequency of the wing in flutter, it is long enough so that the steady state input design can be applied. In the design procedure, the locations of the excitation and the accelerometer are kept fixed, and the input frequency spectrum and power in each frequency of the spectrum are selected.

To simplify the procedure, the parameters in the F, G, and H matrices are identified directly (D does not contain any unknown parameter). The input is designed to produce the most accurate estimates of the underlined parameters in equations (27) and (28) in the sense of minimizing the determinant of the inverse of the information matrix. Starting from the topmost spectrum of figure 3 with available power distributed equally among five frequencies at 2, 4, 6, 8, and 10 cycles per second, the iterative design procedure gives the results shown in the figure. In every iteration, the design procedure adds a new frequency or increases the power at a frequency already included in the spectrum. This leads to a large number of frequencies in the computed spectrum. As mentioned above, this design can be simplified. When frequencies with relative power less than 5 per cent or closer than 0.4 hertz are merged with the neighboring frequencies, the resulting design is shown in figure 4. There are eight frequencies in the optimal spectrum--three each clustered around the two oscillatory modes and one each at a low and an intermediate frequency. Of the three frequencies around the oscillatory modes, one is below, one is above, and one is close to the natural frequency. This characteristic seems to be quite general and substantiates Gerlach's intuitive choice of input frequencies for the identification of the short period parameters of an aircraft (ref. 9). A 2 second time trace for this input spectrum with initial phases selected at random is shown in figure 5.

### Choice of Accelerometer Location

In the flutter analysis of a two dimensional wing, typically only one accelerometer is used. It is generally desired that the best accelerometer within the test budget be selected. There may be a possibility of using two poorer quality accelerometers. This tradeoff was not studied.

The location of this accelerometer is an important parameter. The following performance index is considered:

$$J = \sum_{i=1}^m \left( \frac{\sigma_{\theta_i}}{\theta_i} \right)^2 \quad (31)$$

where  $\theta_i$  ( $i=1,2,\dots,m$ ) is the set of parameters of interest and  $\sigma_{\theta_i}$  is the standard deviation of estimation error in the  $i$ th parameter. Figure 6 shows the values of the performance index for constant input rms value and constant output rms value as a function of the accelerometer position. The minimum of the curves gives the positions of the optimal location of the accelerometer under the two constraints.

#### Simulation and Maximum Likelihood Identification

The flutter equations for the transition matrices of equations (27) to (29) are simulated with the input of figure 5. Both  $\frac{e_o}{c}$  and  $\frac{e_f}{c}$  are taken as 0.1, and the accelerometer rms random error is 0.02 in the nondimensional units. The transfer function between the input and the output is as follows:

$$-0.0155 \frac{(s^4 + 0.360s^3 + 0.599s^2 + 0.208s + 0.0099)}{(s^5 + 0.572s^4 + 0.457s^3 + 0.158s^2 + 0.0292s + 0.00139)} \quad (32)$$

Three identification runs were made:

- (a) The underlined parameters in equations (27) and (28) are estimated. Note that  $H$  is a linear combination of the first two rows of  $F$ . The estimated and the measured time histories are shown in figure 7.
- (b) The input/output relation is represented as a five pole, four zero transfer function. The coefficients of the transfer function are identified directly. This requires estimation of 10 parameters. The measured and estimated time histories of the accelerometer response are shown in figure 8. The match between the two time histories is comparable to that in figure 7. The identified transfer function is

$$-0.0137 \frac{(s^4 + 0.432s^3 + 0.593s^2 + 0.229s + 0.00844)}{(s^5 + 0.525s^4 + 0.451s^3 + 0.145s^2 + 0.0297s + 0.00116)} \quad (33)$$

Certain identifiability problems were indicated by the analysis of the information matrix. This, together with the fact that one zero is very close to a pole (eq. (30)), indicated that a lower order model may be more useful.

- (c) The input/output relationship is represented by a four pole, three zero model. The coefficients of the fourth order transfer function are identified by using the maximum likelihood method. The time history plots are shown in figure 9, and the identified transfer function is as follows:

$$-0.0157 \frac{(s^3 + 0.250s^2 + 0.569s + 0.139)}{(s^4 + 0.467s^3 + 0.400s^2 + 0.119s + 0.0195)} \quad (34)$$

Though the fit to the time history responses is poorer than before, no identifiability problems are indicated, implying that the fourth order transfer function is an adequate representation for the accelerometer output/shaker input relationships. This is also indicated by the plots of the gains and the phases of the fifth order and fourth order identified transfer functions in figures 10 and 11.

The poles and zeros of the transfer function used in the simulation and the identified transfer functions in each of the three cases given above are shown in figures 12 and 13. The closeness of poles and zeros in every case indicates that the poles and zeros of the transfer function can be identified quite accurately and that often lower order models may give as good or better results. It should also be noted that the mode which is poorly damped is identified more accurately than the mode which has higher damping.

#### APPLICATION TO LARGE AEROELASTIC STRUCTURES

A major application of the input design and instrument selection procedures is the estimation of the flutter characteristics of large three dimensional structures. In general, the dynamic flutter behavior of such structures is described by partial differential equations in space and time. For the evaluation of dynamic stability and structural loads, however, a modal analysis or a finite element analysis is sufficiently accurate and converts the more complex partial differential equations into ordinary differential equations. The differential equations describing the flutter characteristics of large structures can be written as follows:

$$\ddot{M}\ddot{x} + \dot{C}\dot{x} + Kx = Du \quad (35)$$



where  $M$  is the generalized mass matrix,  $C$  is the damping matrix,  $K$  is the spring constant matrix, and  $D$  is the input or force distribution matrix. In the vector  $x$ , each term corresponds to a linear or angular displacement of one of the modes. The vector  $u$  is a vector of deterministic or random inputs. There may be unknown parameters in  $M$ ,  $C$ ,  $K$ , and  $D$ . An accelerometer measures acceleration at one point, which, in general, is a linear combination of several components of  $\ddot{x}$ , i.e.,

$$y_a = H_a \ddot{x} \quad (36)$$

where  $H_a$  represents the parameters which determine the locations of the accelerometers. The strain gages measure displacements, so that their outputs are linear combinations of  $x$ , as follows:

$$y_s = H_s x \quad (37)$$

Again,  $H_s$  determines the locations of various strain gages. The locations of the inputs are determined by certain parameters in the matrix  $D$ . The transfer function between  $y_a$  and  $u$  is

$$y_a(s) = s^2 H_a (Ms^2 + Cs + K)^{-1} D u(s) \quad (38)$$

and the transfer function between  $y_s$  and  $u$  is

$$y_s(s) = H_s (Ms^2 + Cs + K)^{-1} D u(s) \quad (39)$$

This multivariable problem can be solved in much the same way as described and demonstrated above. It is currently being applied to a 19-mode model of tilt rotor vehicle for tunnel test.

## CONCLUSIONS

This paper describes how techniques of system identification can be applied to the problem of determining accurate estimates of certain critical parameters in aeroelastic structures.

It was shown that information theoretic approaches can be used for the selection of input spectra and instruments. In particular, various functionals of the inverse of the information matrix provide useful measures of the accuracy of the parameter estimates. The parameter estimation accuracy depends upon both the input spectra and the points where the inputs are applied. The functionals of the inverse of the information matrix can be minimized under practical con-

straints of total cost, the cost versus the accuracy of various available instruments and certain location constraints, the set of instruments which must be used, and the positions at which they should be located can be optimized. In some cases, the instruments are already installed, but the maximum number of channels is fixed because of telemetry, recording, computer capacity, and many other reasons. A tradeoff can be made between various instruments and the possibility of having two or more instruments share one channel.

In the application of system identification methodology to aeroelastic structures, the importance of an efficient parameter identification program cannot be overestimated. A good method based on the maximum likelihood approach that utilizes an eigenvalue analysis of the information matrix provides not only efficient parameter estimates but also important diagnostics regarding the identifiability of various model parameters and the relevance of various models. An aeroelastic analysis of a two dimensional wing, for example, showed that a lower order transfer function may be adequate to represent the input/output relationships.

Maximum utilization of these techniques will, of course, be realized in large aerodynamic structures where identifiability could be a serious problem. Further work in the development of these techniques is under way.

## APPENDIX A

### ALGORITHM FOR CHOOSING OPTIMAL INPUT SPECTRUM

The following procedure may be used to determine the optimal input spectrum:

- (a) Choose a nondegenerate input  $f_o(\omega)$  (i.e., consisting of more than  $\frac{m}{2p}$  frequencies, with a finite power in each frequency).

- (b) Compute the function  $\psi(\omega, f)$  where

$$\psi(\omega, f) = \text{Re}[\text{Tr } R^{-1} \frac{\partial T}{\partial \theta} M^{-1}(f) \frac{\partial T^*}{\partial \theta}] \quad \text{to minimize } |M^{-1}(f)| \quad (\text{A1})$$

$$= \text{Re}[\text{Tr } R^{-1} \frac{\partial T}{\partial \theta} W M^{-2}(f) \frac{\partial T^*}{\partial \theta}] \quad \text{to minimize } \text{Tr}(M^{-1}(f)W) \quad (\text{A2})$$

Find its maximum at  $\omega_o$  under the constraint of equation (13).

- (c) Evaluate the information matrix  $M(\omega_o)$  at  $\omega_o$ .

- (d) Update the design

$$f_1 = (1-\alpha_o) f_o + \alpha_o f(\omega_o) \quad 0 < \alpha_o < 1 \quad (\text{A3})$$

$\alpha_o$  is chosen to minimize  $|M^{-1}(f)|$  or  $\text{Tr}(M^{-1}(f)W)$ , where

$$M(f_1) = (1-\alpha_o) M(f_o) + \alpha_o M(\omega_o), \quad 0 < \alpha_o < 1 \quad (\text{A4})$$

It can be shown that such an  $\alpha_o$  exists.

- (e) Repeat steps (b) through (d) until desired accuracy is obtained.

In the procedure described above, the function  $\psi$  has many local maxima. It is computationally time consuming to find  $\omega_o$  where  $\psi(\omega, f)$  is maximum. In the computer implementation of the algorithm, we consider finite number of values  $\omega_1$  and search through all values of  $\psi(\omega_1)$  to find the maximum. Most stable systems of interest are low pass filters. Thus, in most cases it is possible to find a subset of  $[0, \infty]$ , where the search need be carried out.

There are several ways to see if the input design is close to optimal. These methods use the following criteria:

- (a) The information matrix does not change substantially from one step to the next, or the optimizing function does not improve significantly with iterations.
- (b) The value of  $\alpha_i$  which optimizes the value of the desired function approaches zero. In other words, little power is placed at newly chosen frequencies.
- (c) The maximum value of the function  $\psi_i$  is not much higher than the maximum value for the optimum design (i.e.,  $m$  if we maximize  $|M|$  and  $\text{Tr}(M^{-1}(f^*)W)$  if we minimize  $\text{Tr}(M^{-1}W)$ ).

In our implementation, (a) and (b) are used as the termination criteria and (c) is used as a check.

APPENDIX B: SYMBOLS  
(All Units Are Metric)

$a$	Elastic axis position from leading edge
$a_1$	Gain coefficient of lift response to step change in angle of attack
$a_2$	$=1-a_1$
$a_i$ ( $i=1,2,\dots$ )	Coefficients of transfer function denominator
$A$	State weighting matrix
$A_1,\dots,A_4$	Coefficient matrices defined by equation (2)
$b_1$	Time constant of lift response to step change in angle of attack
$b_2$	$=b_1 c/2V$
$b_i$ ( $i=1,2,\dots$ )	Coefficients of transfer function numerator
$c$	Wing chord
$C$	Cost function of all instruments; generalized damping
$C_i$	Cost coefficient of a single instrument
$d$	Derivative
$D$	Control distribution matrix to measurements; control matrix (equation (35))
$e$	Position of c.g., relative to elastic axis
$e_f$	Distance of force application from elastic axis (positive forward)
$e_o$	Distance of accelerometer from elastic axis (positive forward)
$E$	Energy constraint
$f(\omega)$	Nondegenerate input function
$f_o(\omega)$	Starting guess of $f(\omega)$ for design algorithm
$f_1(\omega)\dots$	Intermediate values of $f_i(\omega)$
$F$	System dynamics matrix; total section lift, input force
$\overline{F}$	$=F/2\pi qS$

G	Control distribution matrix
H	Measurement distribution matrix
H <sub>a</sub>	Accelerometer measurement state distribution matrix
H <sub>s</sub>	Strain gage measurement state distribution matrix
j	$=\sqrt{-1}$
J	Cost functional
k	Reduced frequency, $k=\omega c/2V$
k <sub>y</sub>	Vertical spring rate
k <sub>φ</sub>	Torsional spring rate
k <sub>m</sub>	Mass radius of gyration
K	Generalized spring rate
L <sub>1</sub>	Quarter chord lift
L <sub>2</sub>	Three quarter chord lift
m	Mass; number of parameters in $\theta$
m <sub>1</sub>	Virtual mass
M	Information matrix; generalized mass
M <sub>ij</sub> (ij=1,2,...)	Elements of information matrix
p	Nondimensional distance = $2Vt/c$ ; number of measurement
q	Dynamic pressure = $1/2 \rho V^2$ ; number of frequencies
r	Nondimensional elastic axis position, $r=e/c$
r <sub>o</sub>	Nondimensional location of accelerometer, $r_o=e_o/c$
r <sub>f</sub>	Nondimensional input force location, $r_f=e_f/c$
r <sub>1</sub>	$=a/c - 1/4$
r <sub>2</sub>	$=3/4 - a/c$
r <sub>ij</sub> (i=1,2,...)	Diagonal elements of measurement noise power spectral density matrix

$R$	Measurement noise power spectral density matrix
$R_e$	Real part
$s$	Laplace operator, $\mathcal{L}(d/dp)$
$S$	Wing area = $cb$
$S(\omega, \theta)$	State transfer function
$S_1(\omega, \theta)$	Specification parameter independent part of $S(\omega, \theta)$
$S_2(\omega, \theta)$	Specification parameter dependent part of $S(\omega, \theta)$
$t$	Time
$T$	Time interval (equation (10))
$T(\omega, \theta)$	Output transfer function
$T_1(\omega, \theta)$	Specification parameter independent part of $T(\omega, \theta)$
$T_2(\omega, \theta)$	Specification parameter dependent part of $T(\omega, \theta)$
$u$	Lift coefficient, $L_1/2\pi qS$ ; control variable
$v$	Measurement noise
$V$	Velocity
$w$	Nondimensional vertical displacement, $y/c$
$\dot{w}$	$\hat{y}/c$
$W$	Information matrix weighting matrix
$x$	State
$y$	Measurement vector ( $p \times 1$ ), vertical deflection
$y_a$	Accelerometer measurement
$z$	Deflection at accelerometer location
$\alpha^*$	Power at frequency $\omega_i^*$
$\alpha'$	Cutoff power
$\alpha_o$	Interpolation coefficient for update of the input design
$\beta$	Input locator parameter

$\gamma$	Scalar adjustment factor
$\theta$	Parameter set
$\theta_i$	Parameter of the set
$\hat{\theta}$	Parameter estimate
$\lambda(\omega, \theta)$	$= 1 + \text{Tr}(AS(\omega, \theta)S^*(\omega, \theta))$
$\lambda_i$	Lagrange multiplier
$\mu$	Mass parameter
$\mu_i$	Lagrange multiplier
$\rho$	Air density
$\phi$	Angular displacement
$\phi_1$	Section pitch rate, $\dot{\phi}$
$\phi_i$	Standard deviation of $\hat{\theta}_i$
$\psi(\omega, f)$	Optimization function
$\omega$	Circular frequency
$\omega_o$	Undamped frequency; starting frequency for design algorithm
$\omega_\phi$	Torsional natural frequency = $\sqrt{\frac{k_\phi}{mk_m^2}}$
$\bar{\omega}_y$	Vertical natural frequency = $\sqrt{\frac{k_\phi}{m}}$
$\bar{\omega}_y$	$= \omega_y c / 2V$
$\omega_\phi$	$= \omega_\phi c / 2V$
$\omega_i^*$	Frequencies within $\Delta\omega$
$\omega_i$	Power weighted average of frequencies $\omega_i^*$



## REFERENCES

1. Baird, E. F.; and Clark, W. B.: Recent Developments in Flight Flutter Testing in the United States. Supplement to the Manual on Aeroelasticity, Volume 4, Chapter 10. AGARD Rept. 596, 1972.
2. Rosenbaum, Robert: Survey of Aircraft Subcritical Flight Flutter Testing Methods. NASA CR-132479, Aug. 1974.
3. Waisanen, P. R.; and Perangelo, H. J.: Real Time Flight Flutter Testing Via Z-Transform Analysis Techniques. AIAA Paper 72-784, Aug. 1972.
4. Cole, Henry A., Jr.: On-Line Failure Detection and Damping Measurement of Aerospace Structures by Random Decrement Signatures. NASA CR-2205, Mar. 1973.
5. Houbolt, John C.: Subcritical Flutter Testing and System Identification. NASA CR-132480, Aug. 1974.
6. Gupta, Narendra K.; and Hall, W. Earl, Jr.: Input Design for Identification of Aircraft Stability and Control Derivatives. NASA CR-2493, Feb. 1975.
7. Mehra, Raman K.: Optimal Input Signals for Parameter Estimation in Dynamic Systems - Survey and New Results. IEEE Trans. on Automatic Control, vol. AC-19, Dec. 1974, pp. 753-768.
8. Mehra, Raman K.; and Gupta, Narendra K.: Status of Input Design for Aircraft Parameter Identification. Methods for Aircraft State and Parameter Identification. AGARD-CP-172, Nov. 1974.
9. Gerlach, O. H.: The Determination of Stability Derivatives and Performance Characteristics From Dynamic Manoeuvres. Presented at 38th Meeting of AGARD Flight Mechanics Panel, Toulouse, France, May 1971.

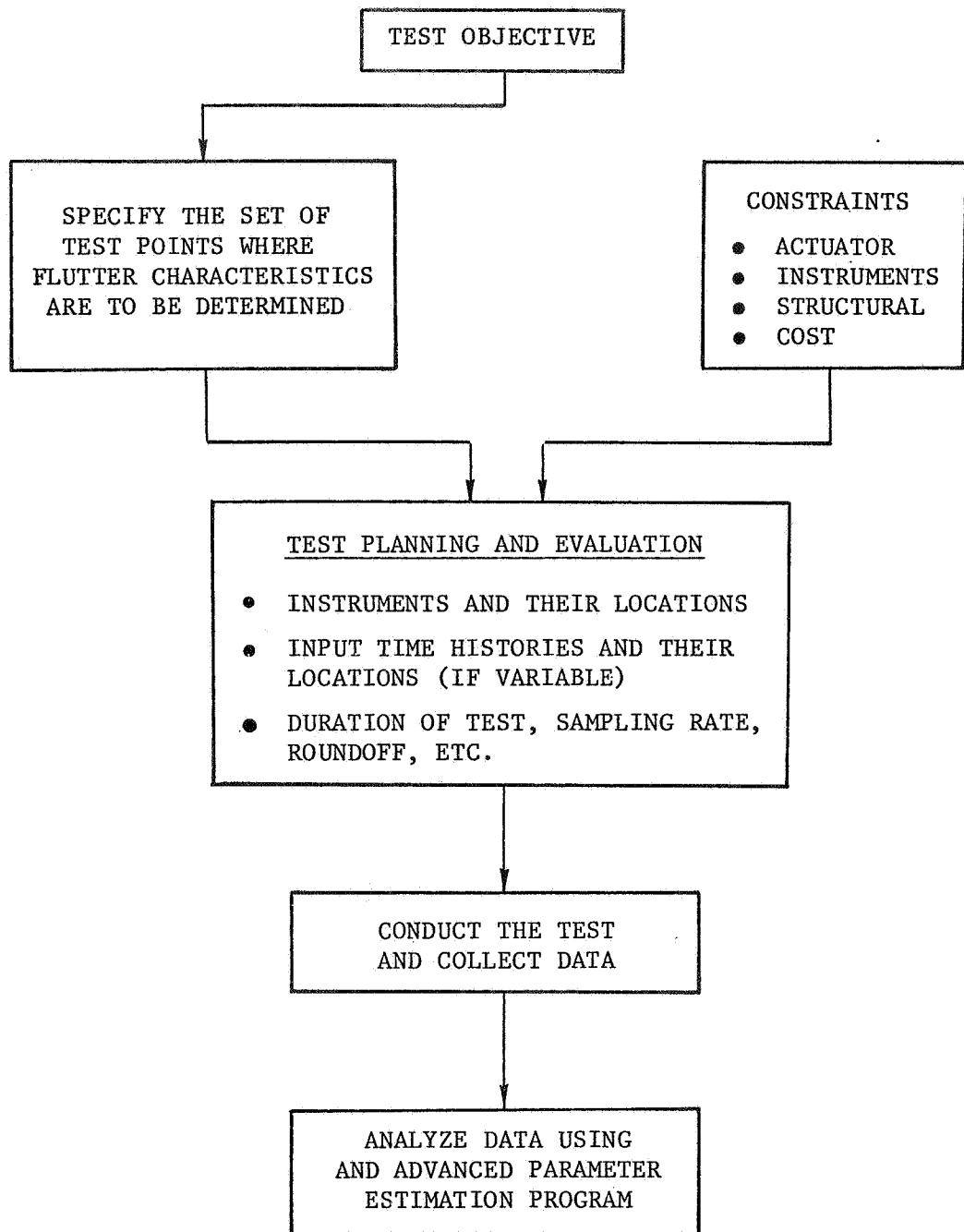


Figure 1. Various steps in aeroelastic testing.



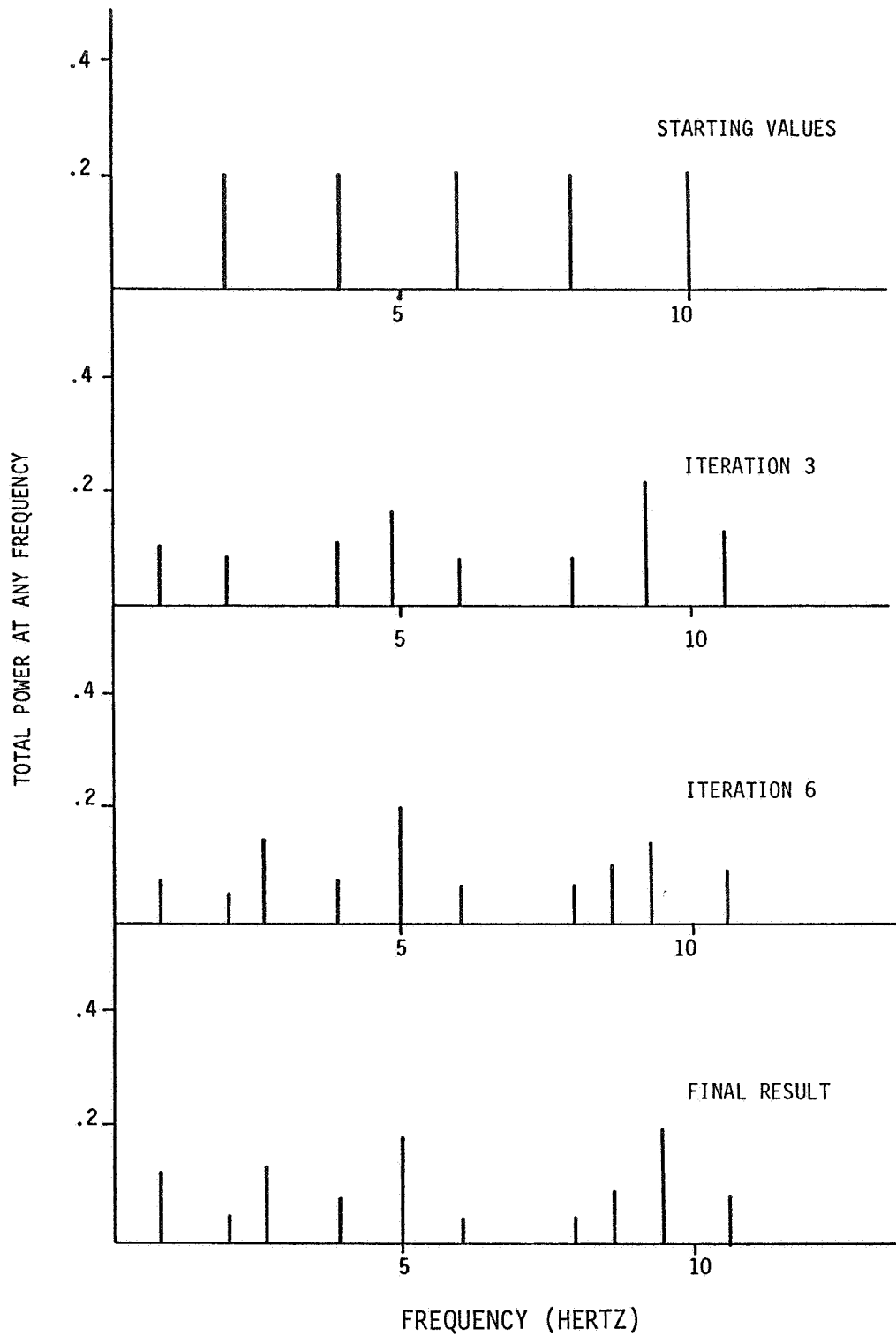


Figure 3. Optimal input design for the identification of flutter parameters.

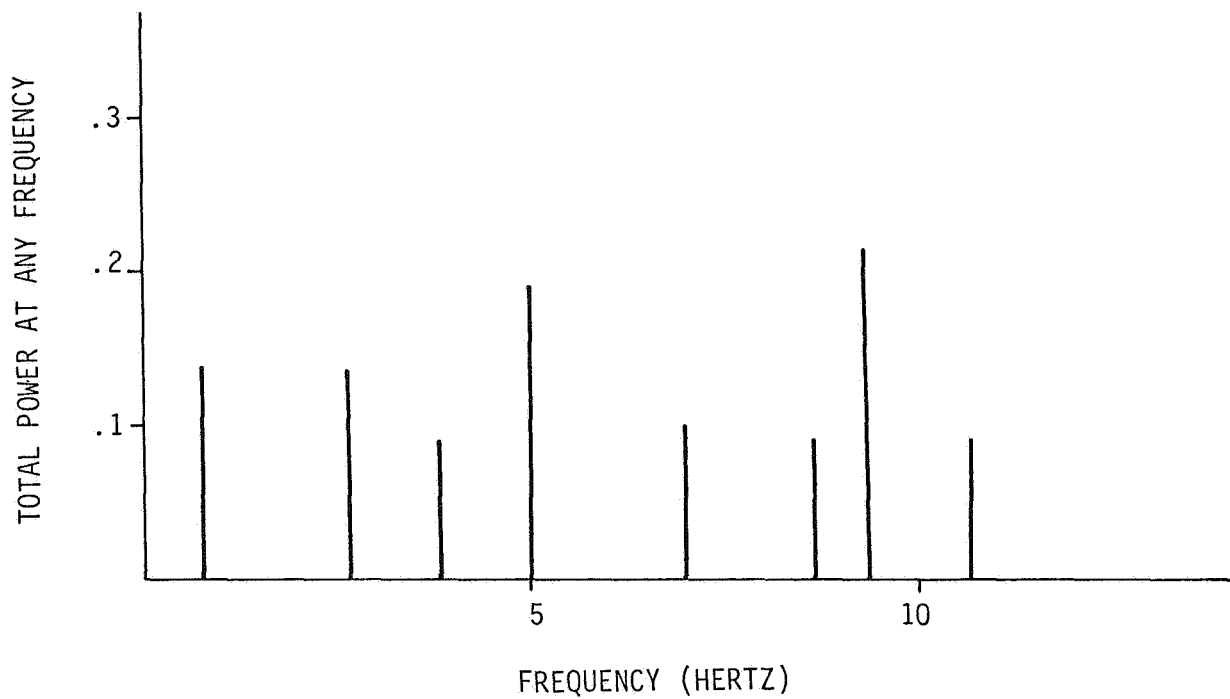


Figure 4. Simplified optimal input spectrum for identification of flutter parameters.

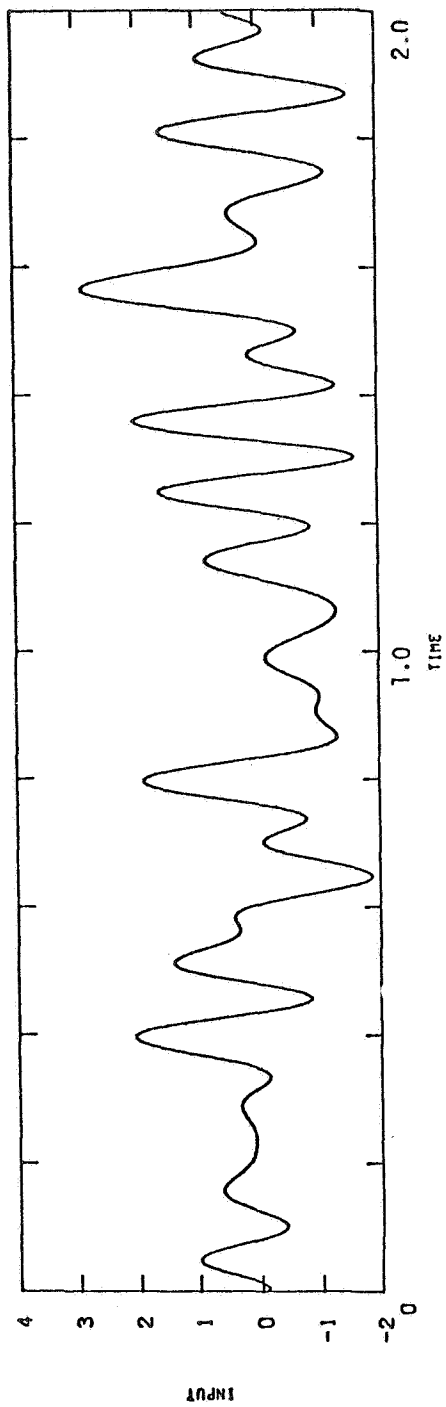


Figure 5. Time history trace of the optimal input.

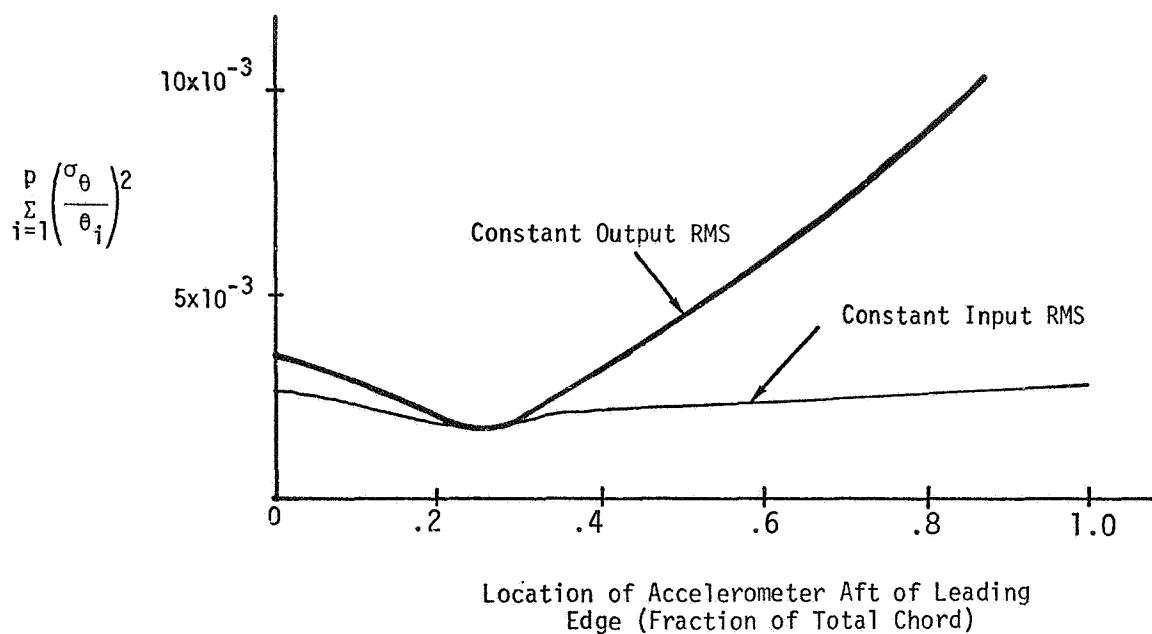


Figure 6. Parameter estimation error as a function of accelerometer position.

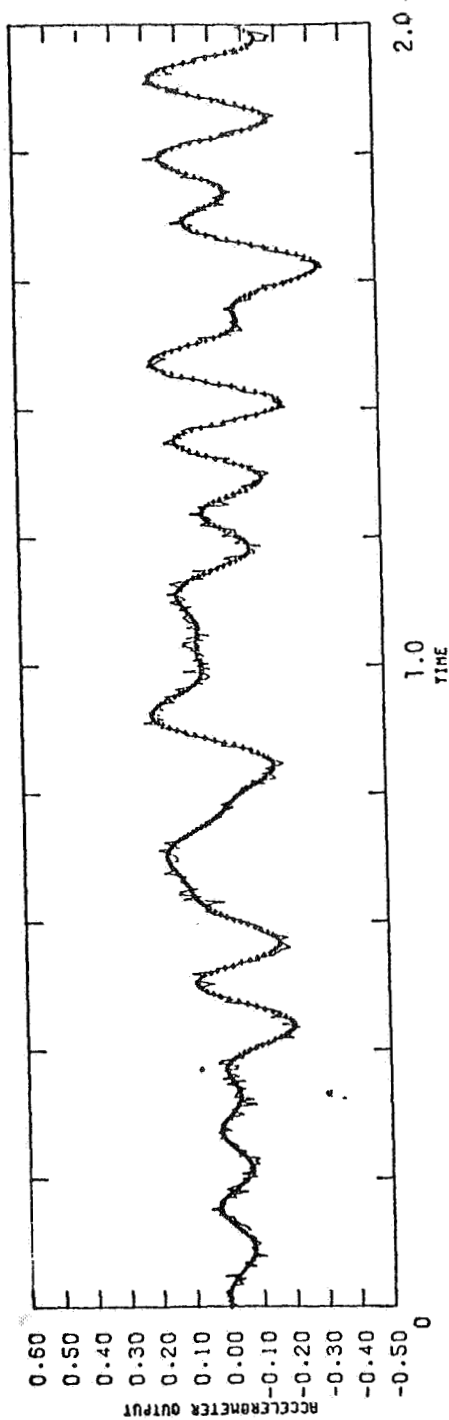


Figure 7. Simulated and estimated time history of the accelerometer output (physical parameters identified).

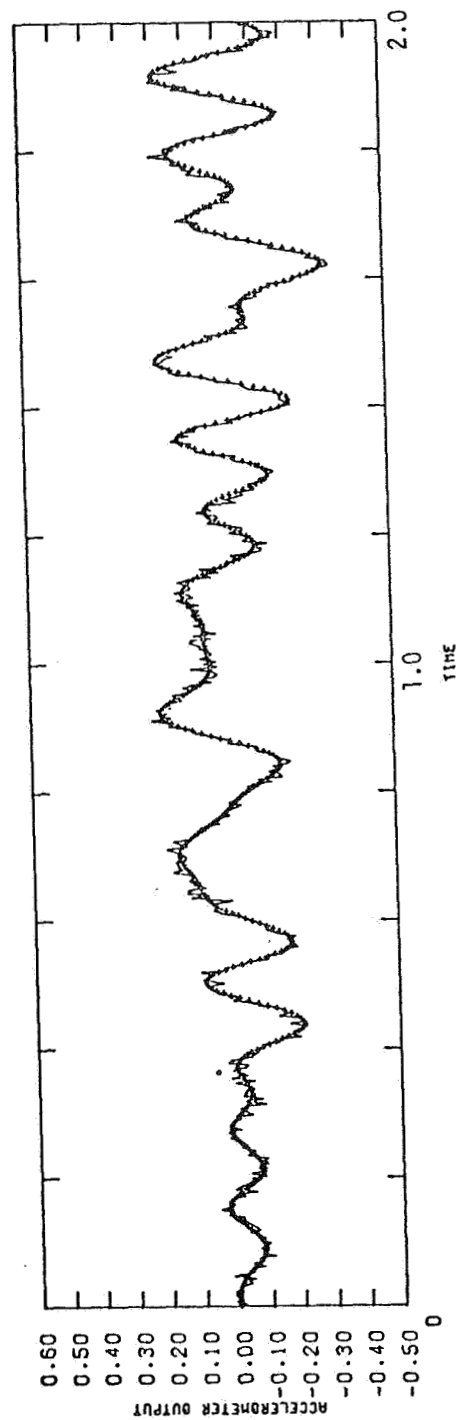


Figure 8. Simulated and estimated time history of the accelerometer output (fifth order transfer function model identified).



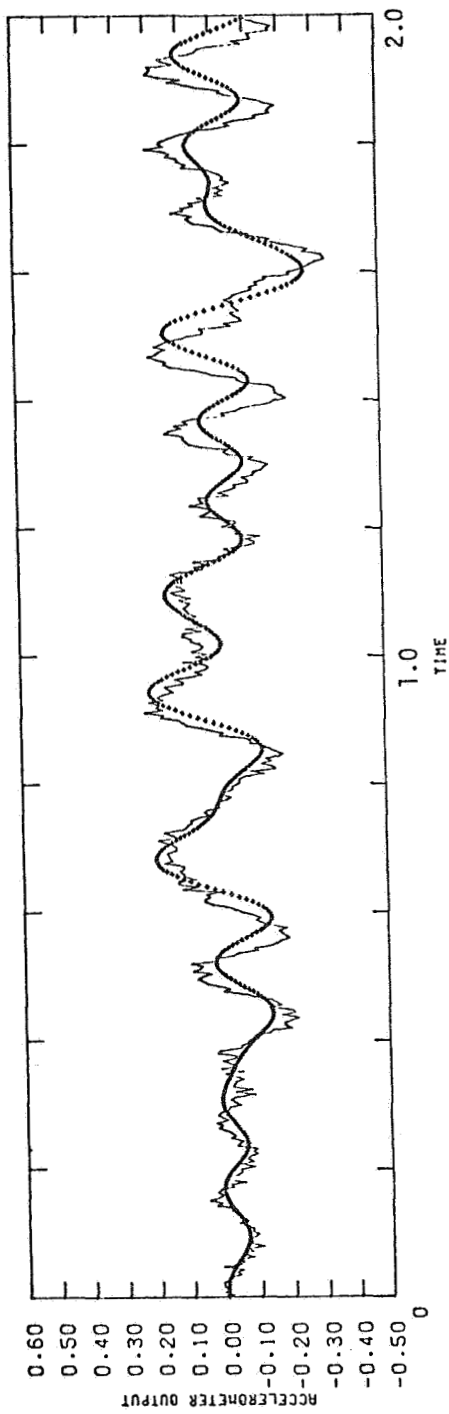


Figure 9. Simulated and estimated time history of the accelerometer output (fourth order transfer function model identified).

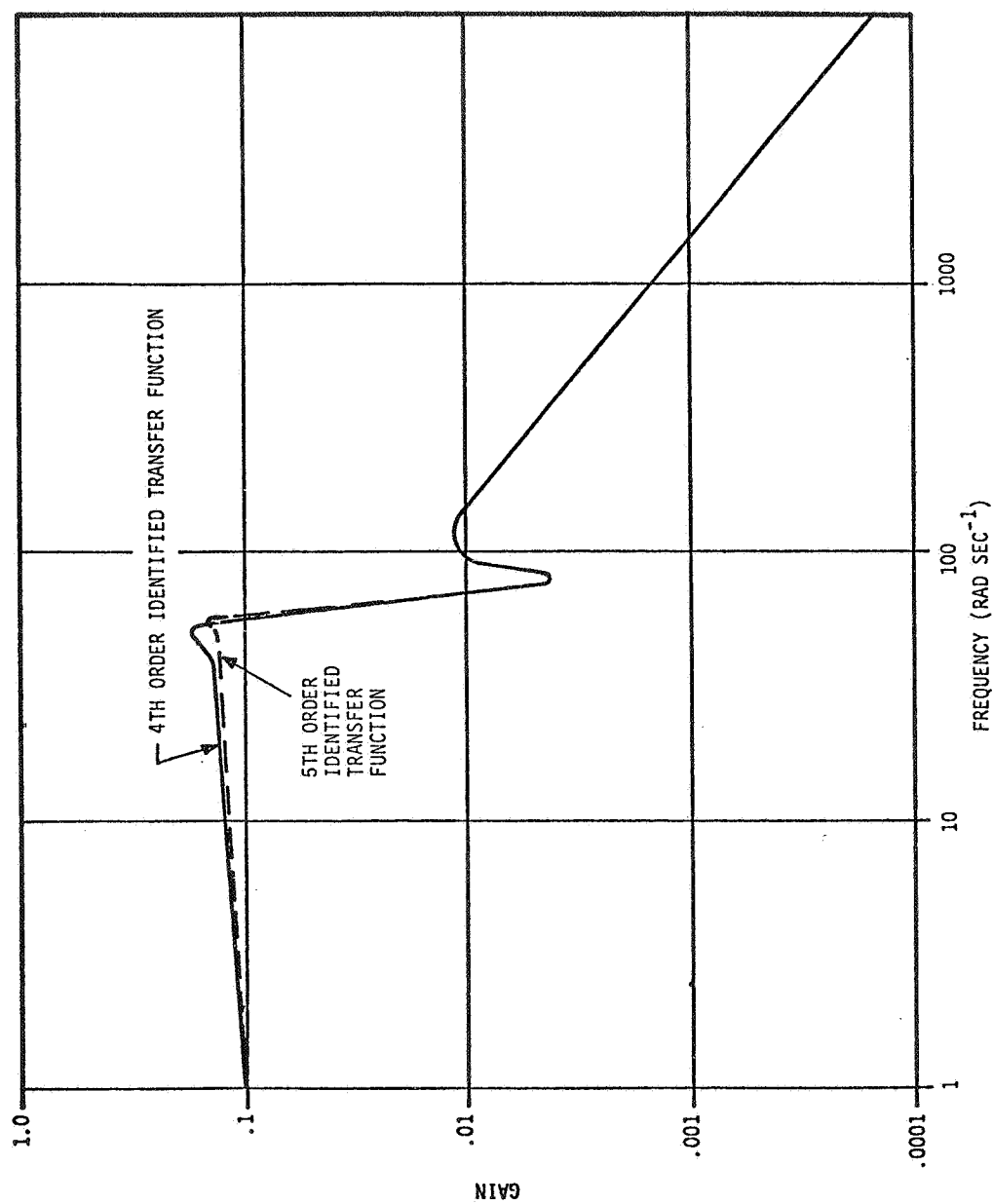


Figure 10. Gain comparisons of fifth order and fourth order identified transfer functions.

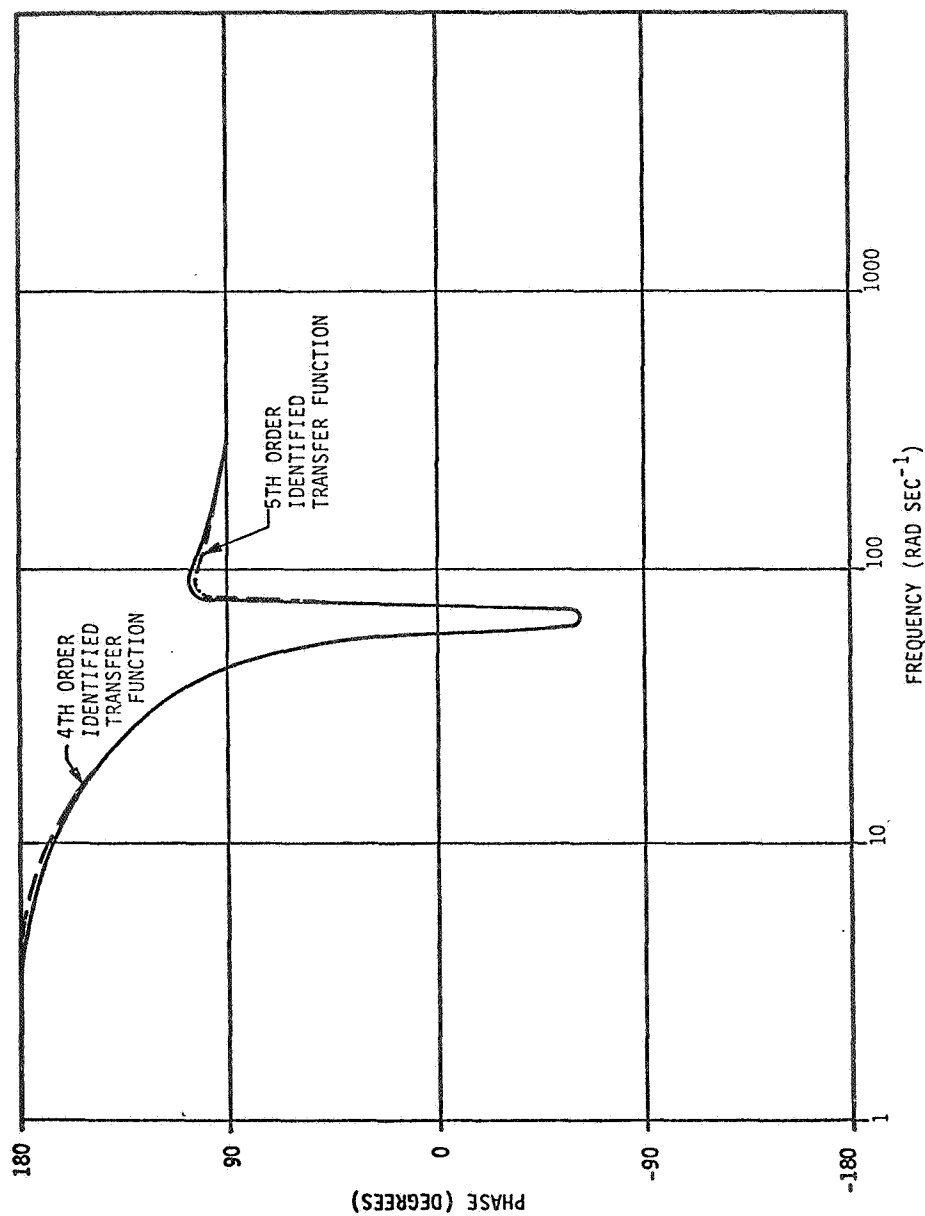


Figure 11. Phase comparisons of fifth order and fourth order identified transfer functions.

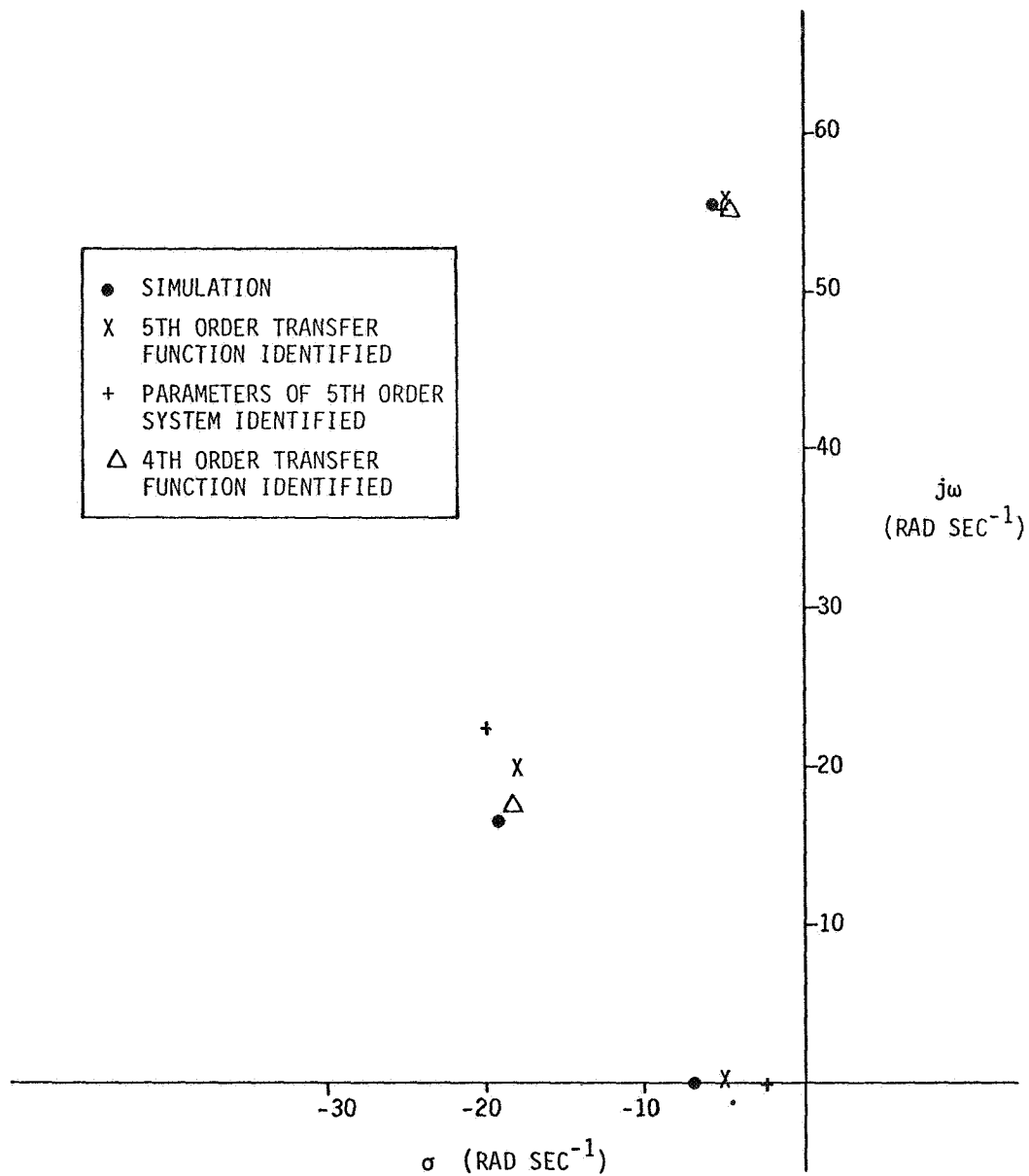


Figure 12. Poles of the simulation transfer function and identified transfer function.

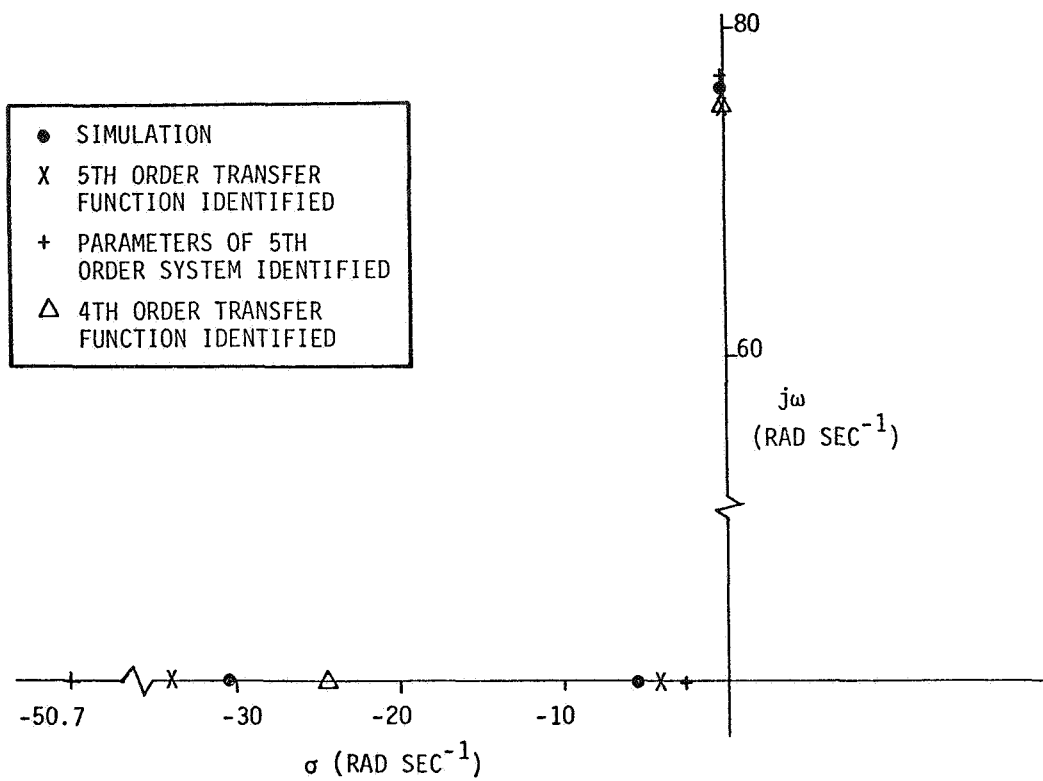


Figure 13. Zeros of simulation transfer function and identified transfer function.